minerals

MDPI

Article

Environmental Pollution Load and Contaminant Transfer in Natura 2000 Protected Brownfield Site

Anja Ilenič [1], Petra Vrhovnik [2], Sonja Lojen [3,4] and Matej Dolenec [5,*]

[1] Department of Materials, Slovenian National Building and Civil Engineering Institute (ZAG), Dimičeva Cesta 12, 1000 Ljubljana, Slovenia; anja.ilenic@zag.si
[2] Institute SeMe, Environmental Awareness and Sustainable Development, Partizanska Street 14, 2319 Poljčane, Slovenia; petra.vrhovnik@outlook.com
[3] Jožef Stefan Institute, Department of Environmental Sciences (JSI), Jamova Cesta 39, 1000 Ljubljana, Slovenia; sonja.lojen@ijs.si
[4] School of Environmental Sciences, University of Nova Gorica, Vipavska 13, 5000 Nova Gorica, Slovenia
[5] Department of Geology, Faculty of Natural Science and Engineering (UL-NTF), University of Ljubljana, Askerčeva Cesta 12, 1000 Ljubljana, Slovenia
* Correspondence: matej.dolenec@ntf.uni-lj.si

Abstract

Revitalisation of contaminated brownfield sites is essential for sustainable development, particularly near sensitive ecological areas like Natura 2000 sites. The lagoon in Slovenia's Regional Park Šturmovci, an artificial wastewater convergence point created during hydroelectric construction, is a highly relevant example. This study integrates geochemical, mineralogical and isotopic analyses to identify sources and controlling mechanisms of contaminant distribution in lagoon sediments and assess their transfer to nearby agricultural soils during flooding events. Results indicate anaerobic conditions, with depth-related shifts in phosphorus, sulphur and redox-sensitive elements, such as rare earth elements (REE), arsenic (As), barium (Ba), cobalt (Co), chromium (Cr), lead (Pb) and vanadium (V), as well as fluctuations in pyrite-rich laminated layers, suggesting potential flood-driven remobilisation of trace elements. Lagoon sediments are highly contaminated with As (73 mg kg^{-1}), Ba (247 mg kg^{-1}), Pb (97 mg kg^{-1}) and Zn (1118 mg kg^{-1}), with elevated concentrations also observed in agricultural soil, all exceeding respective limit values of 20, 160, 85 and 200 mg kg^{-1}. Pollutant concentrations were highest near wastewater inflows and decreased with distance, with nitrogen isotopic patterns indicating partial nitrification and surface ammonium accumulation, reflecting intensive agricultural inputs in the area. High enrichment factor ($EF > 20$) and geoaccumulation index ($I_{geo} > 3$) values, in particular for As, Cd and Zn, indicated severe contamination and highlighted the urgent need for effective remediation strategies, including immobilisation using biochar or cement-based binders, as well as phytoremediation approaches.

Keywords: Natura 2000; pollution; ecological status; brownfield; soil; sediment

Academic Editors: Gevorg Tepanosyan, Silvia Fornasaro and Nosir Shukurov

Received: 2 February 2026
Revised: 7 April 2026
Accepted: 14 April 2026
Published: 21 April 2026

1. Introduction

Brownfields represent a significant environmental and spatial challenge in Europe with an estimated three million sites, 33% of which are contaminated due to past industrial activities. The comprehensive sustainable management strategies for brownfield remediation and revitalisation are hindered due to the absence of a unified definition across the European Union (EU), with only 115,000 sites remediated by 2016 [1–3]. Their regeneration

is essential, particularly where they interfere with sensitive ecological sites, such as the Natura 2000 network. Europe's aquatic and terrestrial environments show poor ecological status. Only 37% of surface water bodies achieved good ecological status, and 61% of soils are unhealthy, mainly due to wastewater and agricultural effluents [1,4]. Although Natura 2000 aims to protect Europe's most valuable species and habitats, many areas remain significantly polluted. Established under the Birds Directive [5] and the Habitats Directive [6], and aligned with the EU Biodiversity Strategy for 2030, the network comprised 27,193 sites in 2022, covering 18.6% of the EU [7]. Anthropogenic contamination has been reported in the Upper Rhine Valley (Germany), Lake Gopło (Poland), Bacau County (Romania) and the Raba River Valley (Hungary), all protected under Natura 2000 [8–11]. Pollution by potentially toxic elements (PTEs) represents a major global problem due to their high potential for bioaccumulation in food chains and subsequent negative impacts on humans and biota [12–14]. Anthropogenic sources contributing PTEs to the environment also include mining, metallurgical and chemical industries, waste disposal and fossil fuel combustion [15–18]. PTEs accumulate in fatty tissues, potentially impair organ and endocrine functions and induce DNA mutations [19,20]. Even at very low concentrations, they can cause severe chronic effects and disrupt the normal functioning of the nervous and cardiovascular systems [14,15]. In addition to human health risks, increased PTE concentrations impair the activity of microorganisms, essential for organic matter decomposition, nutrient cycling and sustaining soil productivity and fertility [15,21]. In addition to PTEs, the pollution load includes various organic micropollutants, such as polycyclic aromatic hydrocarbons, polychlorinated dibenzodioxins/dibenzofurans and phytopharmaceutical agents, all commonly found in nutrient-rich waste streams like municipal sewage sludge, organic and mineral fertilisers, industrial effluents and unmanaged landfill areas [22–25].

Furthermore, one such brownfield site, an artificially created lagoon located in a Natura 2000 protected area, formerly used as a wastewater convergence and contaminated by various organic and inorganic pollutants, was selected for ecological status evaluation. The study addresses the research gap regarding contaminant distribution and mobility, as well as their potential source to agricultural soil transfer, while evaluating associated environmental and health impacts. By linking contaminant patterns in soils and sediments with flooding dynamics and land-use practices, the study provides insights for remediation and sustainable management strategies of brownfield wetlands, where flooding is the primary pathway for contaminant transfer.

2. Materials and Methods

2.1. Study Area

Regional Park Šturmovci is located in the north-eastern part of Slovenia, in the Podravska region, within lowland triangle between Lake Ptuj and Drava and Dravinja rivers. It comprises a 215-hectare remnant of the riparian zone. Geologically, the study area consists of Quaternary flood and alluvial facies, which are interdependent with river fluctuation mechanisms. The Regional Park Šturmovci is strongly influenced by flooding, occurring approximately 10–11 times per year, which significantly affects metal concentrations in the sediments. The central part is characterised by heterogeneous layers of gravel, sand and silt, while the southern part consists of sandy marl, conglomerates, sandstones and sand layers, alternating in an unequal sequence (Figure 1).

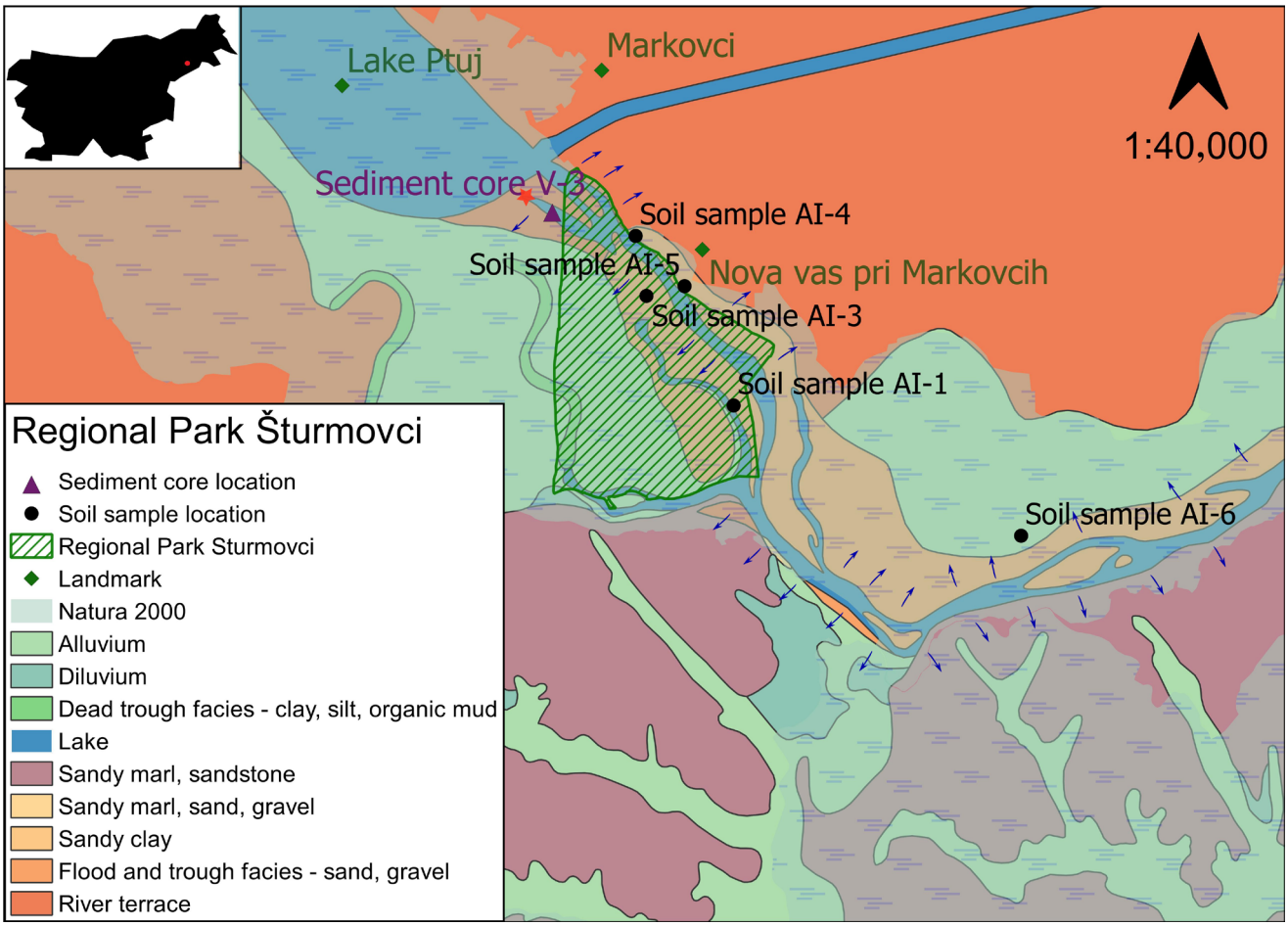

Figure 1. A geological map of Regional Park Šturmovci, pinpointing the locations of collected samples (AI-1, AI-3, AI-4, AI-5, AI-6 and V-3), along with the wastewater inflow point (red star) and flood pathways (small blue arrows) (Adjusted from Mioč and Žnidarčič, 1987 [26]).

The park area is classified as a protected forest of significant natural value and is a part of the Natura 2000 network [27]. However, within the park boundaries, approximately 200 m from the settlements of Nova vas and Markovci, an artificially created lagoon is located. The lagoon was formed during the construction of the nearby Formin hydroelectric power plant in 1978 and served at the time as a convergence point for industrial wastewater from the surrounding area [28–31]. The lagoon, which is about 500 m long, 50 m wide and 2–5 m deep, is predominantly filled with contaminated sludge, with only the uppermost 20 cm consisting of water [28,29,32–34].

2.2. Soil and Sediment Sampling

Pollution load assessment of the Šturmovci lagoon was conducted through detailed geochemical characterisation of sediment and soil samples collected during Spring 2019 (Figure 1). During springtime, river levels are the highest due to the snowmelt in the upper catchment area (in Austria) and more frequent rainfall, maximising the potential to observe flood-related processes. A sedimentary profile (Figure 2), covering the interval from the base of the water column (0 cm) to a depth of 97 cm, was obtained from the deepest part of the lagoon (46°23′8.39″ N, 15°55′34.65″ E) using a gravitational UWITEC coring platform (Mondsee, Austria).

Figure 2. A composite sedimentary profile divided into ten lithological units (0–97 cm).

The sediment core was then divided into ten lithological units based on visual characteristics, including grain size and colour, including silty and medium-grained sand component with lamination, silty and fine-grained sand component, white–green silty lamination, silty and fine-grained sand component, silty lamination, silty and medium-grained sand component, silty component with greenish lamination, silty component with fine-grained sand, silty lamination and silty component. A clear alternation between silty and fine-grained sandy layers with distinctive white–green laminations was observed. In addition, basic physicochemical parameters of the lagoon water, such as pH, temperature and oxidation-reduction potential (ORP), were measured at a depth of 5–10 cm using a SevenGo™ (SG2, Mettler Toledo, Greifensee, Switzerland) multiparameter meter. Five composite soil samples, each assembled from multiple subsamples and homogenised, were taken from the uppermost 20 cm, collected from nearby agricultural fields to evaluate the

potential transfer of contaminated sludge from the lagoon. All samples were dried to a constant mass at +45 °C, homogenised to <0.063 mm and stored at 0 °C for approximately one week prior to geochemical analyses.

2.3. Mineralogical Characterisation

The mineralogical composition was determined for all five soil and ten sediment samples, representing each lithological unit. X-ray diffraction (XRD) analysis was performed using a Philips PW 3710 diffractometer (Eindhoven, The Netherlands) equipped with an automatic aperture, Cu X-ray tube, proportional counter and secondary graphite monochromator. The instrument operated at 40 kV and 30 mA, employing CuKα radiation (λ = 1.54060 Å). Measurements were conducted over a 2θ range of 2–70° at a scanning rate of 3.0° 2θ per minute. Mineral phases were identified using the PAN-ICSD database and the X'Pert HighScore Plus 4.6 software package. Quantitative phase composition was obtained using Rietveld refinement, which ensures optimal agreement between calculated and measured diffractograms. Results are reported to one decimal place, with a detection limit of 0.2%. Mineral abbreviations follow the IUGS international recommendation, based on the updated version of the Kretz (1983) list [35]. To complement the XRD results and confirm mineral presence, additional analyses were performed using a scanning electron microscope with an energy-dispersive spectrometer (SEM-EDS; Thermo Fischer Scientific Quattro S, Waltham, MA, USA). Samples were carbon-coated, and analyses were conducted under high-vacuum conditions at an accelerating voltage of 20 kV and working distance of 10 mm.

2.4. Multielemental Chemical Characterisation

Major and trace elements, including rare-earth elements (REE), were analysed in sediment samples collected from the sedimentary profile of the polluted lagoon. Major elements included aluminium (Al), calcium (Ca), iron (Fe), potassium (K), magnesium (Mg), sodium (Na), phosphorus (P), sulphur (S) and titanium (Ti). Trace elements included silver (Ag), arsenic (As), barium (Ba), cadmium (Cd), cobalt (Co), chromium (Cr), copper (Cu), mercury (Hg), molybdenum (Mo), nickel (Ni), lead (Pb), antimony (Sb), selenium (Se), thallium (Tl), vanadium (V) and zinc (Zn). In addition, trace elements posing the highest potential environmental risk were determined in soil samples from agricultural fields to assess the potential transfer from the lagoon. Microwave-assisted acid digestion (CEM MARS 6) using a mixture of nitric (HNO_3), hydrochloric (HCl) and hydrofluoric (HF) acids in combination with hydrogen peroxide (H_2O_2) was used. Following acid digestion, boric acid (H_3BO_3) was added to the samples to remove fluorides. The clear digests were diluted, and the total elemental concentrations were determined by inductively coupled plasma mass spectrometry (ICP-MS), using certified reference materials STD OREAS25A4A, STD OREAS45E and STD DS11, alongside replicates and blank measurements to ensure accuracy and precision. The method's limit of detection (MDL) for specific elements was as follows: for 0.01%, 0.01%, 0.01%, 0.01%, 0.01%, 0.001%, 0.001%, 0.04% and 0.001% for Al, Ca, Fe, K, Mg, Na, P, S and Ti, respectively. The MDLs for trace elements were as follows: for 20 ppb, 0.2 ppm, 1 ppm, 0.02 ppm, 0.2 ppm, 1 ppm, 0.1 ppm, 0.01 ppm, 0.05 ppm, 0.1 ppm, 0.02 ppm, 0.02 ppm, 0.3 ppm, 0.05 ppm, 1 ppm and 0.02 ppm for Ag, As, Ba, Cd, Co, Cr, Cu, Hg, Mo, Ni, Pb, Sb, Se, Tl, V and Zn, respectively. The MDLs for REEs were 0.1 ppm. The analytical uncertainty was better than 3%, and precision was ±10%.

2.5. Isotopic Composition of Nitrogen

The isotopic composition of nitrogen ($\delta^{15}N$) was determined in three soil and seven sediment samples from a sedimentary profile to evaluate potential ^{15}N enrichment resulting from anthropogenic inputs, including wastewater discharge and agricultural fertiliser

applications, in order to identify potential nitrogen sources within the ecosystem. An isotope ratio mass spectrometer (Europa 20–20; Sercon Ltd., Crewe, UK) with a preparatory module ANCA-SL was used, with results for $\delta^{15}N$ reported as relative δ (delta) values (Equation (1)) per mille (‰), according to

$$\delta^{15}N[‰] = \frac{R_{sample} - R_{standard}}{R_{standard}} \times 1000 \quad (1)$$

where R is the ratio of heavy to light isotopes ($^{15}N/^{14}N$) of the sample and standard (atmospheric nitrogen—N_2). To ensure quality assurance and quality control, the following commercially available laboratory isotope standards were used: urea (50 µg C ml^{-1}), protein (Casein) Organic Analytical Standard (Cat no. B2155—Certificate no. 114859), Sorghum flour Organic Analytical Standard (Cat no. B2159—Batch no. 257737) and wheat flour Organic Analytical Standard (Cat no. B2157—Batch no. 114855). Measurement determined from repeated sample analyses was ±0.15‰.

2.6. Data Analysis and Environmental Pollution Load Assessment

Statistical analyses and data visualisation were performed using Statistica 13.3, Grapher 11 and Surfer 8.0 [36–38], as well as Draw.io online software (29.6.6). Basic statistical parameters (minimum, maximum, mean, median, standard deviation, skewness, kurtosis and range) were calculated, and data normality was evaluated using histograms and distribution metrics. Due to predominantly non-normal data distribution and small sample size, non-parametric tests were applied, including Mann–Whitney tests and Spearman's correlation coefficients, at a significance level of $\alpha < 0.05$. Environmental load was assessed by calculating the enrichment factor (*EF*) and geoaccumulation index (I_{geo}). *EF* (Equation (2)) was calculated as

$$EF = \frac{\frac{PTE}{RE}_{sample}}{\frac{PTE}{RE}_{background}} \quad (2)$$

with the ratio between the studied element and a reference element (RE) [39]. Al is commonly used as the primary RE due to its stability, association with clay minerals and resistance to weathering processes [12]. However, due to the presence of the local aluminium industry, Fe and manganese (Mn) were selected as reference elements. They are relatively immobile and minimally affected by anthropogenic sources, making them conservative choices with minimal variability between the two. Background values were derived from elemental concentrations in the upper continental crust [40]. *EF* values ranging from 0 to 1.5 indicate PTE's natural origin, whereas values exceeding 1.5 suggest potential anthropogenic influence [41]. Based on *EF*, soils are categorised into minimal ($EF < 2$), moderate ($EF < 5$), considerable ($EF < 20$), very high ($EF < 40$) and extremely high enrichment ($EF > 40$) with PTE [12]. I_{geo} (Equation (3)) was evaluated according to

$$I_{geo} = log_2 \frac{c_{sample}}{1.5 \times c_{reference}} \quad (3)$$

where c_{sample} represents the concentration of PTE in the sample, and $c_{reference}$ denotes its concentration in the reference material [42]. Factor 1.5 is used to minimise the natural variations in the environment. Concentrations of the PTEs in the upper continental crust were used as reference values [40]. Soils with I_{geo} values near 0 are classified as unpolluted, those with values of 1–2 moderately polluted, 3–5 highly polluted and $I_{geo} > 5$ as extremely polluted [42]. In addition, concentration values were compared with the Slovenian threshold, warning and critical soil limit values [43]. For elements not covered by the Slovenian

regulation, comparisons were made with Dutch target, intervention and contamination thresholds [44], as well as EU Council Directive 86/278/EEC [45].

3. Results and Discussion

3.1. Mineralogical Composition and Phase Distribution

The mineralogical composition of soil and lagoon sediments is similar (Figures 3 and 4) and reflects the geological background of the study area. Silicate minerals are predominant (Ab—albite, Am—amphibole, An—anorthite, Clc—clinochlore, Ms—muscovite), followed by carbonates (Cal—calcite, Dol—dolomite), oxides and hydroxides (Bhm—boehmite, Hem—hematite, Qtz—quartz), as well as sulphides (Py—pyrite) and phosphates (Viv—vivianite). Noticeable differences were observed only for Am, An, Py and Viv, which occurred mainly in the lagoon silt sediments.

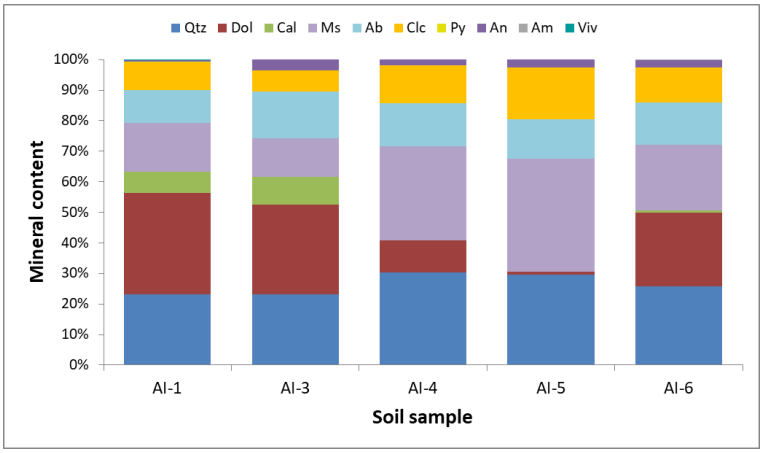

Figure 3. Mineral composition of the soil samples.

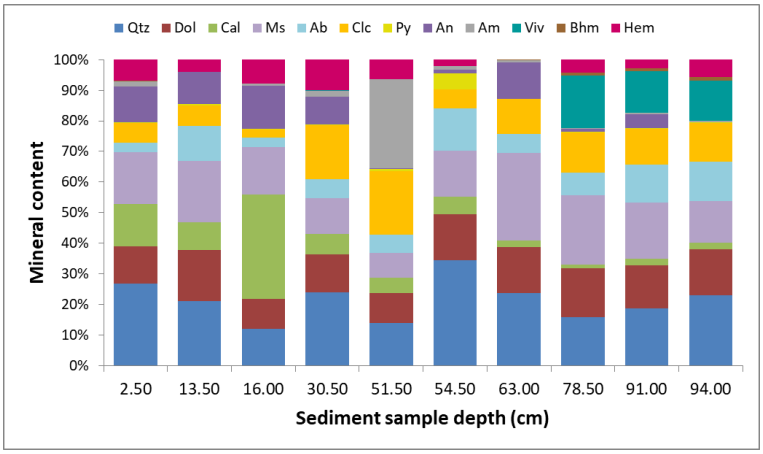

Figure 4. Mineral composition of the sediment core, highlighting the noticeable variations in Am, An, Py and Viv; indicative of reducing, organic matter and Fe-enriched conditions characteristic of contaminated environments.

Bhm (Figure 5a) was detected in the north-western part of the lagoon, near the point of wastewater inflow, and in the deepest sediment layers, where highest pH and lowest ORP values were observed, ranging from 7.27 to 7.55 and from −29 mV to −13 mV, respectively. Overall, the lagoon area is characterised with slightly basic and strongly anoxic conditions, which favours the elevated concentrations of Viv and Pyr.

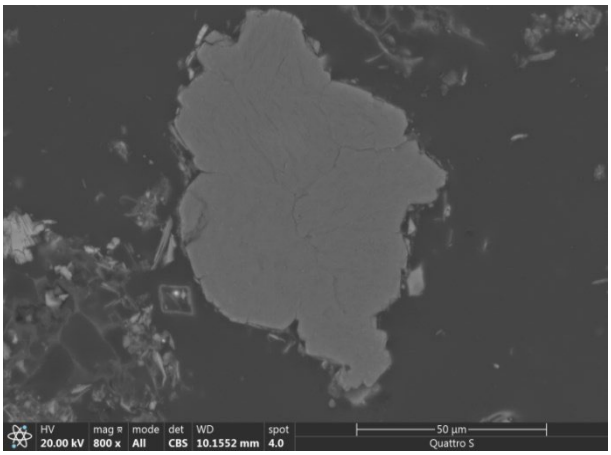

(**a**)

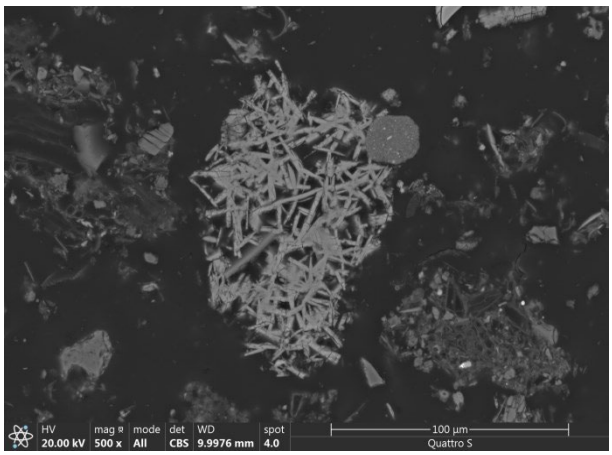

(**b**)

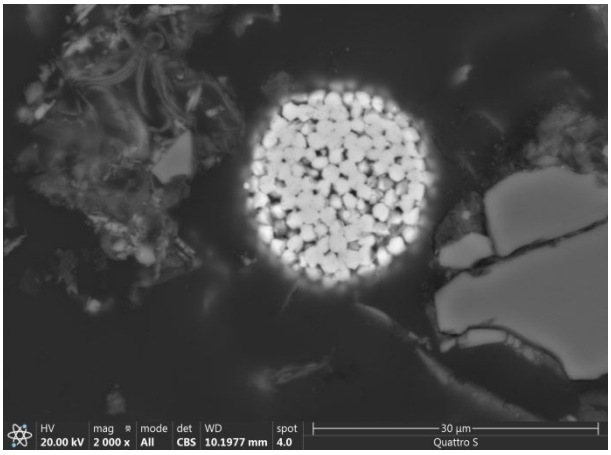

(**c**)

Figure 5. SEM-EDS figures of Bhm (**a**), Viv (**b**) and Pyr (**c**), respectively.

Viv (Figure 5b) minerals typically form in anaerobic environments, where not all Fe is utilised in sulphide mineral formation. These conditions are generally found in sediment with sulphur (S)-to-Fe ratio < 1.5 [46]. Authigenic Viv occurs in reducing environments rich in organic matter and Fe, conditions found in the vicinity of wastewater treatment plants or areas receiving high inputs of nutrients [46].

3.2. Geochemical Composition of Sediment and Soil Samples

Concentrations of major elements in the lagoon sediments, decreased in the following order: Al > Fe > Ca > P > Mg > S > K > Na > Ti (Table 1). At a depth of 62.5–63.5 cm notable change was observed, with increase in Al, Ca, Mg and Ti and decrease in P and S.

Table 1. Concentrations of major elements (%) in lagoon sediment samples.

Depth (cm)	Al	Ca	Fe	K	Mg	Na	P	S	Ti
4.0–5.0	6.00	6.97	2.97	0.98	2.06	0.60	1.03	0.87	0.20
10.0–11.0	5.17	5.31	1.82	0.54	0.96	0.39	2.23	0.92	0.16
15.5–16.5	7.31	7.63	2.51	0.36	0.65	0.24	2.32	0.94	0.11
21.0–22.0	8.93	4.30	3.60	0.37	0.72	0.30	1.97	1.11	0.12
27.0–28.0	8.11	4.50	2.99	0.32	0.68	0.26	2.03	1.37	0.11
33.0–34.0	9.58	3.80	3.63	0.38	0.82	0.34	1.54	1.17	0.12
39.0–40.0	7.83	3.78	4.56	0.40	0.82	0.34	1.96	1.32	0.13

Table 1. *Cont.*

Depth (cm)	Al	Ca	Fe	K	Mg	Na	P	S	Ti
45.0–46.0	7.16	4.04	4.52	0.42	0.87	0.36	1.45	1.74	0.12
51.0–52.0	8.51	3.97	3.75	0.35	0.83	0.30	1.34	1.80	0.12
58.0–59.0	4.59	4.22	5.23	0.73	1.24	0.64	0.56	1.88	0.16
62.5–63.5	7.24	4.48	4.30	1.80	2.38	0.92	0.30	0.49	0.38
69.0–70.0	4.60	3.47	8.62	0.76	1.34	0.49	2.05	0.92	0.15
75.0–76.0	4.90	3.12	10.21	0.65	1.24	0.40	1.92	0.72	0.13
81.0–82.0	5.62	3.32	9.46	0.72	1.36	0.49	1.85	0.79	0.14
90.5–91.5	5.54	3.55	7.94	0.81	1.45	0.51	1.66	0.63	0.16
93.5–94.5	5.44	3.37	7.88	0.77	1.35	0.47	1.65	0.68	0.15

A similar pattern was observed for PTEs at this depth, where the concentrations of Ba, Co, Cr, Pb and V increased, while Ni exhibited a decrease. Generally, PTEs decreased in the following order: Zn > Ba > Cu > Pb > Cr > As > V > Ni > Mo > Co >Ag > Cd > Se > Sb > Tl > Hg (Table 2).

Table 2. Concentrations of PTEs (mg kg^{-1}) in lagoon sediment samples.

Depth (cm)	Ag	As	Ba	Cd	Co	Cr	Cu	Hg	Mo	Ni	Pb	Sb	Se	Tl	V	Zn
4.0–5.0	1.76	41.9	212	6.70	10.60	83.0	176	1.15	11.6	53.5	349	1.85	2.90	2.66	71.0	1840
10.0–11.0	0.34	37.6	145	5.06	7.20	82.0	214	1.75	24.8	76.5	141	2.20	4.60	3.03	119	2007
15.5–16.5	0.74	75.2	420	1.19	7.10	45.0	151	1.22	12.4	49.6	47.5	1.24	2.50	1.10	80.0	1177
21.0–22.0	3.76	44.4	294	3.12	8.60	59.0	208	1.99	13.9	78.3	90.6	2.05	3.60	2.98	64.0	1343
27.0–28.0	9.07	40.1	208	2.58	7.00	50.0	291	1.95	12.2	60.0	81.3	2.36	3.70	1.68	50.0	1863
33.0–34.0	4.49	46.4	282	1.81	6.60	63.0	146	1.48	10.6	75.9	75.8	1.81	3.00	1.80	50.0	1058
39.0–40.0	10.9	91.2	143	2.21	6.30	103	185	1.72	13.6	82.0	77.4	2.34	4.00	1.91	54.0	1358
45.0–46.0	14.4	78.0	103	2.31	5.90	127	168	2.04	12.3	122	82.6	2.65	3.20	2.36	54.0	1381
51.0–52.0	9.90	91.2	128	3.44	6.50	87.0	262	2.89	13.8	197	80.6	3.84	4.00	4.73	73.0	1633
58.0–59.0	4.25	136	58	1.95	7.40	71.0	150	1.65	15.6	45.5	83.1	5.53	2.70	2.95	49.0	950
62.5–63.5	1.23	45.2	955	4.00	16.10	109	75.5	1.02	4.41	55.5	286	2.46	1.50	3.00	105	1054
69.0–70.0	1.67	106	149	3.68	7.20	77.0	120	0.66	6.86	46.1	118	4.05	2.70	2.85	59.0	973
75.0–76.0	1.23	129	346	3.83	7.60	79.0	135	0.72	5.75	46.5	109	3.85	3.20	2.80	66.0	1020
81.0–82.0	1.22	89.9	330	3.83	7.30	74.0	105	0.67	5.76	48.8	103	3.26	2.40	2.93	57.0	957
90.5–91.5	1.31	62.8	339	3.50	8.70	82.0	102	0.79	3.94	43.8	134	3.55	2.10	3.21	60.0	966
93.5–94.5	1.10	70.4	310	3.76	7.30	80.0	106	0.73	4.42	44.6	116	3.46	2.90	2.98	56.0	908
[43]:																
Limit value	nd	20	nd	1	20	100	60	nd	10	50	85	nd	nd	nd	nd	200
Target value	nd	30	nd	2	50	150	100	nd	40	70	100	nd	nd	nd	nd	300
Critical value	nd	55	nd	12	240	380	300	nd	200	210	530	nd	nd	nd	nd	700
[44]:																
Target value	nd	nd	160	nd	nd	nd	nd	nd	nd	nd	nd	3	0.7	1	42	nd
Intervention value	nd	nd	625	nd	nd	nd	nd	nd	nd	nd	nd	15	nd	nd	nd	nd
Serious pollution	15	nd	nd	nd	nd	nd	nd	nd	nd	nd	nd	nd	100	15	250	nd
[45]:																
Minimum	nd	nd	nd	nd	nd	nd	nd	1	nd	nd	nd	nd	nd	nd	nd	nd
Maximum	nd	nd	nd	nd	nd	nd	nd	1.5	nd	nd	nd	nd	nd	nd	nd	nd

Orange values exceed limit values, purple values exceed alert values, and red values exceed critical values; nd denotes values not determined. In cases where Slovenian legislation does not provide limit values, reference values from [44,45] were used.

At this depth, a corresponding change in the sedimentary profile was also observed (Figure 2), with more dominant appearance of a thicker layer of white–green lamination. In addition, the grain size transitions from medium to fine-grained, accompanied by an increase in Pyr content (up to 5.3%) (Figures 4 and 5c).

This trend is further supported by the distribution of REEs (Figure 6), which can be classified into light REE (LREE; La–Sm) and heavy REE (HREE; Dy–Yb). In this study, REEs varied from 0.07 mg kg^{-1} to 106.44 mg kg^{-1}, with the highest concentrations observed for Ce, La and Nd. The highest REE concentrations occurred at depths 15.5–16.5 cm and

62.5–63.5 cm. The LREE/HREE ratio varied between 3.03 and 7.79, with the greatest differences at these depths. All REEs exhibited statistically significant positive correlation with K, Mg and Ti and statistically significant negative correlation with S. REE concentrations were normalised to UCC and chondrite to assess the geochemical anomalies. Chondrite-normalised patterns showed a strong LREE enrichment with a decreasing trend toward the HREE, consistent with weathering processes. UCC-normalised patterns confirmed enrichment at 16 cm and 63 cm, indicative of significant anthropogenic input due to potential remobilisation of material during flooding events.

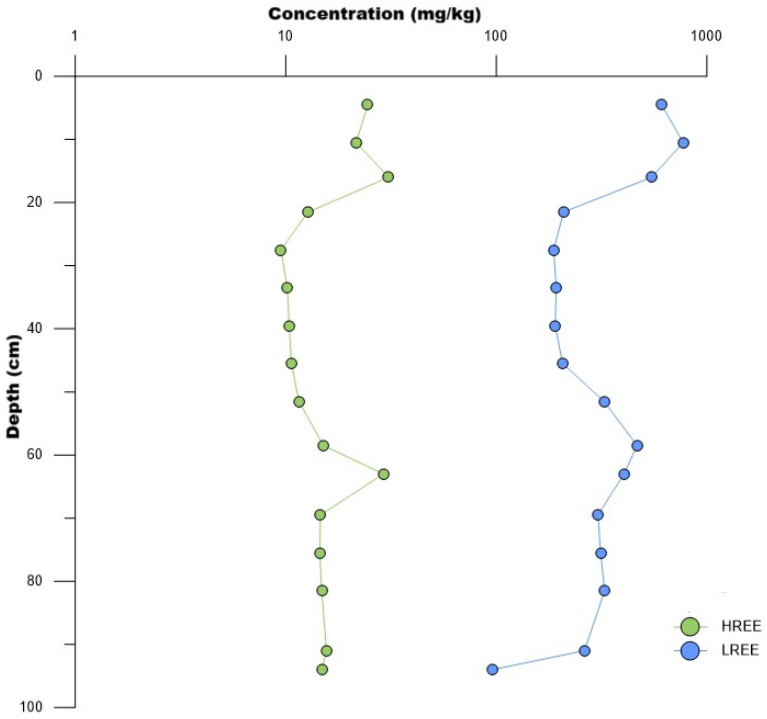

Figure 6. Depth-dependent variation in total HREE and LREE concentrations, with two elevated intervals suggesting enhanced material remobilisation, potentially associated with flooding events.

These variations can indicate alternating reducing and oxidising conditions, which strongly influence the remobilisation and increased availability of trace elements, potentially driven by flooding events, which are frequent in the Regional Park Šturmovci [47,48]. The elements most sensitive to redox conditions are primarily As, Co, Cu, Mo, Ni, Se, V, Zn and REE [14,49]. Under anaerobic conditions, reductive dissolution of Fe and Mn hydroxides can occur, primarily controlled by pH, salinity, organic matter content and temperature [47]. This process also promotes the release of As, Cd, Cr, Co, Cu, Fe, Mn, Mo, Ni, Pb, V and Zn from solid to aqueous phases [14,50]. Sediments may become enriched with specific PTEs due to upstream anthropogenic inputs, followed by their adsorption and potential infiltration through the soil profile during remobilisation after prolonged flooding [51,52]. Enrichment at depths of 16.00 and 63.00 cm can reflect the two major flood events that occurred after the construction of the Formin hydropower plant, one in 1998 and one in 2012, consistent with a silt sedimentation rate of 2.5–3.0 cm year^{-1}. In both cases, the Drava River flooded due to high precipitation levels in Austria. Peak discharges reached 1.650 m^3 s^{-1} and 3.165 m^3 s^{-1} in 1998 and 2012, respectively [53–55]. During the flooding event, concentrations of Cd, Pb and Zn exceeded the critical limit values [56].

Based on the Spearman correlation coefficients (Figure 7), the PTEs can be grouped into two sub-categories according to their potential origin: (i) Ag, Co, Cu, Hg, Mo, Ni, Se and Zn and (ii) Cd, Co, Pb and Ti. The first group shows a strong correlation with S, suggesting the

influence of sulphate-reducing microorganisms and the formation of authigenic sulphide minerals, which are characteristic of reducing environments [57,58]. Microbial sulphate reduction is one of the primary pathways for sulphide mineral formation in anaerobic settings [59]. Sulphates may be introduced into the environment via floodwaters or formed during the decomposition of organic matter [60]. However, future studies are needed to fully assess the role of microbial processes in mineral formation. The second group shows a strong positive correlation with K, Mg, Na and Mn and a negative correlation with S, indicating an association with elements predominantly found in silicate minerals (feldspars, micas, amphiboles) characteristic of fluvial and alluvial facies. Furthermore, a decrease in P, likely due to uptake by microorganisms, may also reflect the flooding events, which strongly influence the transport and accumulation of pollutants. These correlations indicate potential associations but do not imply direct causality, and further research is needed to confirm the associated mechanisms.

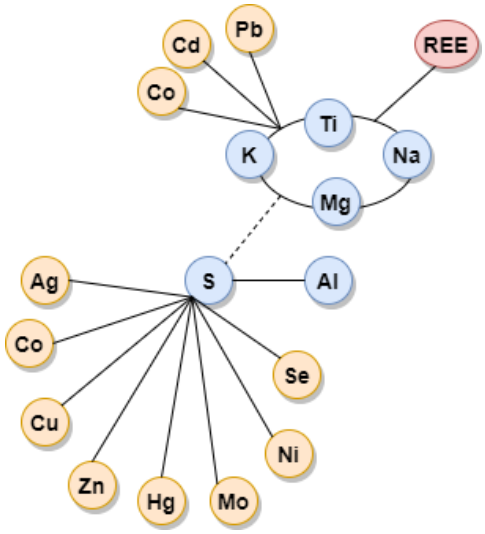

Figure 7. Diagram of Spearman correlation coefficients (>0.7), with dashed line indicating negative correlation. Two groups are identified based on their potential origin: (i) phases associated with sulphate-reducing microorganism introduced via wastewater or formed during organic matter decomposition and (ii) silicate minerals characteristic of fluvial and alluvial facies.

In addition, to assess the potential transfer of contaminated material from the lagoon to surrounding areas, PTE concentrations in agricultural fields were also analysed (Table 3). The Regional Park Šturmovci is flooded approximately 10–11 times a year, heavily impacting the metals concentrations. Mann–Whitney tests revealed no statistically significant differences between locations for most elements, except for As, Cu and Mo. The median As concentration in five agricultural soil samples was 34 mg kg^{-1}, exceeding the limit of 20 mg kg^{-1} at all locations. Median Cu and Mo values were 52 mg kg^{-1} and 2 mg kg^{-1}, respectively, both below their limit values of 60 mg kg^{-1} (Cu) and 10 mg kg^{-1} (Mo).

Median concentrations of As, Cd, Cu, Mo, Ni, Sb and Zn were higher in lagoon sediments, while Ba, Pb and V were more elevated in agricultural soils. These differences may result from the application of fertilisers and phytopharmaceutical agents, variations in geological substrate and material redistribution during frequent flooding. The highest PTE concentrations were found at site AI-3, nearest to the contaminated lagoon, and the lowest at site AI-4 on the opposite side of the Drava River, indicating downstream pollutant transport.

Table 3. Concentrations of PTEs (mg kg^{-1}) in agricultural soil samples.

Soil Sample	As	Ba	Cd	Cr	Cu	Mo	Ni	Pb	Sb	V	Zn
AI-1	40	1841	9	82	34	4	152	790	2	92	2643
AI-3	47	2960	14	82	37	6	153	1096	2	82	3110
AI-4	21	641	1	106	52	1	73	92	1	124	259
AI-5	34	831	1	143	69	2	77	104	2	167	284
AI-6	27	752	3	102	60	2	67	306	2	121	915
[43]:											
Limit value	20	nd	1	100	60	10	50	85	nd	nd	200
Target value	30	nd	2	150	100	40	70	100	nd	nd	300
Critical value	55	nd	12	380	300	200	210	530	nd	nd	700
[44]:											
Target value	nd	160	nd	nd	nd	nd	nd	nd	3	42	nd
Intervention value	nd	625	nd	nd	nd	nd	nd	nd	15	nd	nd
Serious pollution	nd	nd	nd	nd	nd	nd	nd	nd	nd	250	nd

Orange values exceed limit values, purple values exceed alert values, and red values exceed critical values; nd denotes values not determined. In cases where Slovenian legislation does not provide limit values, reference values from [44,45] were used.

3.3. Assessment of the Isotopic Composition of Nitrogen ($\delta^{15}N$)

In soils where nitrogen is derived from biologically fixed atmospheric N_2, $\delta^{15}N$ values are typically around 0‰. Higher $\delta^{15}N$ values may result from enhanced organic matter decomposition or anthropogenic inputs from fertilisers, animal waste or municipal and industrial wastewaters [61–64]. Overall, $\delta^{15}N$ values increased with distance from the wastewater inflow point (Table 4); however, $\delta^{15}N$ data alone are insufficient to accurately distinguish or quantify potential nitrogen sources. Soil cultivation and fertiliser application, which replenish nitrogen losses, exert a strong influence on $\delta^{15}N$ values [64]. The $\delta^{15}N$ values of inorganic fertilisers are similar to those of atmospheric N_2, as they are produced through reactions of H_2 with atmospheric N_2 [62,63,65]. For organic fertilisers and animal waste, higher $\delta^{15}N$ values (around +9‰) are typical, resulting from the increased input of ^{15}N-enriched ammonia (NH_3^+) and nitrate (NO_3^-) compounds [62–65]. $\delta^{15}N$ values of various animal wastes are generally similar: poultry waste ranges from +1 to +10‰, pig waste from +6 to +37‰ and mixed-animal waste from 0 to +11‰. N_{total} is typically higher in poultry waste due to protein supplements in feed. $\delta^{15}N$ values of municipal waste range from −4 to +10‰ [65]. ^{15}N values also change with depth, where upper values are enriched with ^{15}N (0–4.5‰), which may result from mixing of soil layers, soil aeration or the volatilisation of ^{15}N-depleted NH_3 following periods of intensive fertilisation [65]. $\delta^{15}N$ values generally increase with depth due to fractionation during N transport, accumulation of ^{14}N in surface layers and ^{15}N at depth via microbial activity, nitrogen uptake by plants or mixing of soil layers [64,66,67]. Decomposition, organic matter content and microbial activity also increase with depth, potentially influencing N patterns [62,66]. At the Šturmovci lagoon, however, a slight decrease in $\delta^{15}N$ was observed, with $\delta^{15}N$ ranging from 3.14‰ to 2.37‰. This pattern may reflect high N inputs from fertilisers and wastewater, promoting partial nitrification and downward leaching of ^{15}N-depleted NO_3^-, while ^{15}N-enriched ammonium accumulates near the surface where it easily is adsorbed on mineral surfaces (e.g., clay minerals, (oxy)hydroxides) and assimilated by plants as a primary nitrogen source [68–70]. For a detailed interpretation, more data on N sedimentary N species distribution and $\delta^{15}N$ depth profiles with higher resolution would be needed; however, this would be beyond the scope of the present study.

Table 4. Isotopic composition of nitrogen in selected soil and sediment samples.

	Location	δ^{15}N (‰)
Soil sample	AI-3	2.00
	AI-5	6.43
	AI-6	4.26
	Depth (cm)	δ^{15}N (‰)
Sediment sample	7.0–8.0	3.14
	18.0–19.0	2.53
	36.0–37.0	2.49
	66.0–67.0	2.89
	84.0–85.0	2.37

3.4. Environmental Pollution Load Assessment

The greatest environmental burden posed by the contaminated lagoon sediments is linked to elevated concentrations of As, Ba, Cd, Cu, Hg, Ni, Pb and Zn, all of which exceeded the critical or alert thresholds for soils and sediments defined in Slovenian legislation [43]. For elements not regulated at the national level, including Ag, Ba, Hg, Sb, Se, Tl and V, measured concentrations were evaluated against reference values provided in [44,45]. Elevated concentrations of As, Ba, Hg and Zn exceeded the critical threshold values, likely reflecting the influence of intensive agricultural activities, including the use of fertilisers and phytopharmaceuticals. The presence of an aluminium industry and a meat-processing plant in the immediate vicinity of the Regional Park Šturmovci may also influence local PTE concentrations. An additional contributing factor is the application of sludge from wastewater treatment plants. In the surrounding area, As and Zn levels are particularly elevated livestock operations (pig and poultry farms), where these elements are commonly added to feed to promote animal growth [18,65,67,71,72]. The chemical composition of sewage sludge is largely determined by the characteristics of the wastewater inputs; however, it typically exhibits high concentrations of Zn, Pb, Cu, Mn and Cr, followed by Ni, B and Mo [25]. The concentrations of PTEs in the lagoon sediments correspond well with typical reported values. Compared to sludge analyses from the Ptuj wastewater treatment plant in 2015, most element concentrations were lower, with the exception of Cu and Zn values [73]. Furthermore, inorganic fertilisers generally have a limited influence on PTE variability in soils and sediments, whereas organic fertilisers can increase Cd, Cr and Zn concentrations [74]. As, Cd, Co, Cr and Mo detected in the contaminated lagoon sediments were found to be comparable to those reported for organic fertilisers [25,74–76]. Moreover, preliminary analyses conducted in 2005 and 2010 indicated environmental contamination with N, Ag, As, Be, Cd, Cr, Cu, Mo, Pb, Tl, V and Zn, with PTE concentrations in this study being substantially higher, indicating progressive contaminant accumulation in the area [28,77]. To assess the potential transport of contaminated sediments during flooding, agricultural soils were also analysed. Concentrations of As, Ba, Cd, Cr, Cu, Pb, Ni and Zn exceeded regulatory limits, with the highest values observed for Cd, Pb and Zn. Compared to other European agricultural areas, soil samples from the Regional Park Šturmovci exhibited elevated contamination levels [71]. While a direct comparison of the measured concentrations with regulatory limit values provides an initial critical assessment of the lagoon's condition, further evaluation was carried out through the calculation of environmental indicators, including *EF* and I_{geo}, according to (Equations (2) and (3)). *EF* calculations for the sediment samples indicated very high to extreme enrichment ($EF > 20$) for Se, Ag, As, Hg, Cd, Zn, Sb, Mo and Cu, generally increasing with depth. The most concerning PTE levels in agricultural soils were observed for As, Cd, Pb and Zn, as confirmed by I_{geo} calculations ($I_{geo} > 3$). In addition, As, Ba, Cd,

Cr, Cu, Hg, Mo, Ni, Pb, Sb, Se, Tl, V and Zn exceeded the regulatory limit values in the lagoon sediments, while As, Ba, Cd, Cr, Cu, Ni, Pb, V and Zn were above the limit values in agricultural soils. Among all, As, Cd, Pb and Zn represent the highest risk due to their high toxicity, long-term environmental accumulation and bioavailability. The results suggest that effective remediation strategies are essential for protecting public health and local biota. Calculated *EF* and I_{geo} values suggest that REE concentrations are unlikely to pose notable environmental and human health risks. Both measured concentrations and environmental factors were highest in the north-western part of the lagoon, where wastewater inflows, and gradually decreased towards the point where lagoon water discharges into the Drava River. Therefore, it can be concluded that the lagoon sediment samples and the surrounding agricultural soils are influenced by wastewater discharges [28,31–34].

3.5. Remediation Potential of the Contaminated Material

Approximately 22,000 m^3 of contaminated sediment require remediation, along with measures to prevent wastewater inflow from the right-bank ditch directly into the lagoon [28,31,33]. Previous evaluations concluded that the most effective approach would be ex situ remediation with dehydration of polluted silt using hydrocyclone, which would reduce both the amount of organic matter containing PTEs and the overall volume of the sediment, as well as successfully immobilise the PTEs [18,28,31]. Due to high organic matter content and fine-grained sediments, the method would require pre-treatment (e.g., flocculation, coagulation, pre-sedimentation) to prevent clogging. In addition to ex situ remediation methods, the toxicity and bioavailability of PTEs can also be mitigated using binding agents such as biochar or zeolites or through phytoremediation with hyperaccumulating plants. Methods employing biochar or zeolites are cost-effective and well-studied, with their effectiveness largely dependent on material properties, application strategies, environmental conditions (e.g., pH, temperature), and pollutant concentrations [78]. High organic matter content can reduce zeolite sorption efficiency, while biochar can enhance soil quality and water retention; with high PTE concentrations (e.g., As, Pb, Zn) requiring higher quantities of biochar. In addition, cement binders can be used as they immobilise multiple metals simultaneously, including those forming soluble hydroxide or silicate complexes, reducing the potential leachability into the groundwater and allowing the stabilised sediment to be reused in embankments or lagoon restoration structures. Phytoremediation represents a sustainable approach, with pollutants removed through mechanisms such as phytostimulation, phytostabilisation, phytovolatilisation, phytodegradation or phytoextraction [79]. Crucifers (*Brassicaceae*) are considered most useful as they can uptake As, Pb, Zn, Cd and Ni efficiently. They are very tolerant to anaerobic and variable conditions, while their roots can stabilise the sediments and prevent re-suspension of polluted materials during floods, as well as limit the leachability into the groundwater.

4. Conclusions

The anthropogenically contaminated brownfield site—lagoon in the Regional Park Šturmovci (Slovenia)—was formed during the construction of a nearby hydroelectric power plant, serving as a convergence point for industrial wastewater from the surrounding area. It is part of the Natura 2000 network. Despite its protected status, the site shows significant environmental degradation, posing potential risks to wildlife and human health. This study provides a comprehensive geochemical characterisation and assesses the potential transfer of materials. The lagoon exhibits anaerobic conditions with vivianite and pyrite, indicative of highly nutrient reducing environments. The chemical assessment reveals pronounced depth-related changes, with a decrease in P and S and an increase in redox-sensitive elements such as REE, As, Ba, Co, Cr, Pb and V. The presence of a thicker white–green

laminated layer with finer grains and higher pyrite content indicates alternating redox conditions. These variations may promote the remobilisation and enhanced availability of trace elements, potentially driven by flooding events. Two sedimentary enrichments likely correspond to floods in 1998 and 2012, consistent with a silt sedimentation rate of 2.5–3.0 cm year^{-1}. The greatest environmental burden is attributed to the contaminated lagoon sediments, associated with elevated concentrations of As, Ba, Pb and Zn, which, at some locations, exceed the critical thresholds defined by Slovenian legislation. PTE concentrations generally decline with distance from the wastewater inflow, a pattern also observed in surrounding agricultural soils. While similar chemical patterns in the lagoon sediments and soils are consistent with possible contaminant transfer during flooding events, alternative contributions from agricultural activities cannot be excluded. Nitrogen isotopic patterns can indicate high nitrogen inputs, potentially reflecting contributions from fertilisers and wastewater, promoting partial nitrification and downward leaching of ^{15}N-depleted nitrate, while ^{15}N-enriched ammonium accumulates near the surface and is preferentially assimilated by plants. The extent of contamination was further assessed using environmental indicators, including *EF* and I_{geo}, whose elevated values confirm severe pollution and highlight the critical state of the site and concurrent urgent need for effective remediation strategies. These findings suggest that ongoing monitoring and targeted sustainable, cost-effective and efficient remediation strategies are essential to support the long-term ecological status of the lagoon within the Natura 2000 network.

Author Contributions: Conceptualisation, A.I., P.V. and M.D.; methodology, A.I., P.V., S.L. and M.D.; data analysis, A.I. and M.D.; writing—original draft preparation, A.I.; writing—review and editing, A.I., M.D., S.L. and P.V.; visualisation, A.I. and M.D.; supervision, M.D. and P.V. All authors have read and agreed to the published version of the manuscript.

Funding: This work was supported by the Slovenian Research Agency (P2-0273, P1-0195, P1-0143 and J7-60124). In addition, this paper was supported by the ReInd-BBG project (DRP0200087), funded under the Interreg Danube Region Programme and co-funded by the European Union.

Data Availability Statement: All data will be made available upon request.

Conflicts of Interest: The authors declare no conflicts of interest.

References

1. European Environment Agency. Progress in the Management of Contaminated Sites in Europe. Available online: https://www.eea.europa.eu/en/analysis/indicators/progress-in-the-management-of (accessed on 6 November 2025).
2. Panagos, P.; Van Liedekerke, M.; Yigini, Y.; Montanarella, L. Contaminated Sites in Europe: Review of the Current Situation Based on Data Collected through a European Network. *J. Environ. Public Health* **2013**, *1*, 158764. [CrossRef]
3. Rizzo, E.; Pesce, M.; Pizzol, L.; Alexandrescu, F.M.; Giubilato, E.; Critto, A.; Marcomini, A.; Bartke, S. Brownfield regeneration in Europe: Identifying stakeholder perceptions, concerns, attitudes and information needs. *Land Use Policy* **2015**, *48*, 437–453. [CrossRef]
4. Joint Research Centre. A New Tool Maps the State of Soil Health Across Europe—The Joint Research Centre: EU Science Hub. Available online: https://joint-research-centre.ec.europa.eu/jrc-news-and-updates/new-tool-maps-state-soil-health-across-europe-2023-03-13_en (accessed on 20 November 2025).
5. Directive 79/409/EEC of the Council of 2 April 1979 on the conservation of wild birds. *Off. J. Eur. Communities* **1979**, *103*, 1979.
6. Council Directive 92/43/EEC of 21 May 1992 on the conservation of natural habitats and of wild fauna and flora. *Off. J. Eur. Union* **1992**, *206*, 50.
7. European Commission. Natura. 2000. Available online: https://environment.ec.europa.eu/topics/nature-and-biodiversity/natura-2000_en (accessed on 20 November 2025).
8. Bontas, B.I.; Mirila, D.C.; Gritcu, G.; NIstor, I.D.; Ureche, D. High Pollution with Heavy Metals NATURA 2000 Protected Area in Bacau County, Eastern Romania. *Rev. Chim.* **2020**, *71*, 154–169. [CrossRef]
9. Juśkiewicz, W.; Gierszewski, P. Toxic metal pollution of aquatic ecosystems of European Union nature protection areas in a region of intensive agriculture (Lake Gopło, Poland). *Aquat. Sci.* **2022**, *84*, 52. [CrossRef]

10. Mauser, K.M.; Wolfram, J.; Spaak, J.W.; Honert, C.; Brühl, C.A. Current-use pesticides in vegetation, topsoil and water reveal contaminated landscapes of the Upper Rhine Valley, Germany. *Commun. Earth Environ.* **2025**, *6*, 166. [CrossRef]
11. Sobczyk, W.; Kowalska, A.; Sobczyk, E.J. Impact Assessment of Sand and Gravel Deposits Mining in Klaj on the Natural Environment of the Raba Rivervalley. *Inżynieria Miner.* **2016**, *17*, 241–248. Available online: https://inz-min.online/index.php/im/article/view/1544 (accessed on 18 November 2025). [CrossRef]
12. Barbieri, M. The Importance of Enrichment Factor (EF) and Geoaccumulation Index (Igeo) to Evaluate the Soil Contamination. *J. Geol. Geophys.* **2016**, *5*, 237–240. [CrossRef]
13. Mateo-Sagast, J.; Marjani Zadeh, S.; Turral, H.; Burke, J. *Water Pollution from Agriculture: A Global Review*; FAO: Rome, Italy, 2017; p. 35.
14. Shaheen, S.M.; El-Naggar, A.; Antoniadis, V.; Moghanm, F.S.; Zhang, Z.; Tsang, D.C.W.; Ok, Y.S.; Rinklebe, J. Release of toxic elements in fishpond sediments under dynamic redox conditions: Assessing the potential environmental risk for a safe management of fisheries systems and degraded waterlogged sediments. *J. Environ. Manag.* **2020**, *255*, 109778. [CrossRef]
15. Bansal, O.P. The Influence of Potentially Toxic Elements on Soil Biological and Chemical Properties. In *Metals in Soil—Contamination and Remediation*; IntechOpen: London, UK, 2018. Available online: https://www.intechopen.com/chapters/63832 (accessed on 4 March 2020).
16. Nawab, J.; Ghani, J.; Khan, S.; Xiaoping, W. Minimizing the risk to human health due to the ingestion of arsenic and toxic metals in vegetables by the application of biochar, farmyard manure and peat moss. *J. Environ. Manag.* **2018**, *214*, 172–183. [CrossRef]
17. Roussiez, V.; Probst, A.; Probst, J.C. Significance of floods in metal dynamics and export in a small agricultural catchment. *J. Hydrol.* **2013**, *499*, 71–81. [CrossRef]
18. Wuana, R.A.; Okieimen, F.E. Heavy Metals in Contaminated Soils: A Review of Sources, Chemistry, Risks and Best Available Strategies for Remediation. *Int. Sch. Res. Not.* **2011**, *1*, 402647. [CrossRef]
19. Briffa, J.; Sinagra, E.; Blundell, R. Heavy metal pollution in the environment and their toxicological effects on humans. *Heliyon* **2020**, *6*, e04691. [CrossRef] [PubMed]
20. Sah, D.; Verma, P.K.; Kandikonda, M.K.; Lakhani, A. Pollution characteristics, human health risk through multiple exposure pathways, and source apportionment of heavy metals in PM10 at Indo-Gangetic site. *Urban Clim.* **2019**, *27*, 149–162. [CrossRef]
21. Li, Q.; Jiao, X.; Busso, C. Impacts of sewage irrigation on soil properties of a farmland in China: A review. *Int. J. Exp. Bot.* **2018**, *87*, 1–21.
22. Charlesworth, S.M.; Booth, C.A. *Urban Pollution: Science and Management*; Wiley: Oxford, UK, 2019; p. 464.
23. Järup, L. Hazards of heavy metal contamination. *Br. Med. Bull.* **2003**, *68*, 167–182. [CrossRef]
24. Khalid, S.; Shahid, M.; Khan Niazi, N.; Murtaza, B.; Bibi, I.; Dumat, C. A comparison of technologies for remediation of heavy metal contaminated soils. *J. Geochem. Explor.* **2016**, *182*, 247–268. [CrossRef]
25. Senesil, G.S.; Baldassarre, G.; Senesi, N.; Radina, B. Trace element inputs into soils by anthropogenic activities and implications for human health. *Chemosphere* **1999**, *39*, 343–377. [CrossRef]
26. Mioč, P.; Žnidarčič, M. *Osnovna Geološka Karta SFRJ 1:100.000—List Maribor in Leibnitz*; Zvezni geološki zavod: Beograd, Serbia, 1987.
27. ARSO (Slovenian Environment Agency). Atlas Okolja. 2020. Available online: http://gis.arso.gov.si/atlasokolja/profile.aspx?id=Atlas_Okolja_AXL@Arso (accessed on 16 February 2020).
28. Ignjatović, M.; Pocajt, S. Sanacija lagune Šturmovci s čiščenjem onesnažene zemlje in vodnih sedimentov. *Ekolist-Revija o Okolju* **2010**, 27–29.
29. Levanič, M. Markovci: Kdo bo saniral ekološko nevarno laguno? *Štajerski Tedn.* **2017**, *70*, 2–3.
30. Ozimec, M. Onesnaževalce lagune bodo ovadili! *Štajerski Tedn.* **2014**, *67*, 5.
31. SLOG-I.I. *Ekološka Sanacija Lagune Šturmovci z Oblikovanjem Predloga za Čiščenje, Obdelavo Sedimentov ter za Vzpostavitev Nadaljnje Trajnostne Rabe Vodnega Telesa ob Upoštevanju Specifik Varovanega Območja*; SLOG-I.I.: Maribor, Slovenia, 2012; p. 34.
32. Meznarič, S. Dokazano strupena laguna v Šturmovcih: Prvič javno razkrita ekološka bomba. *Štajerski Tedn.* **2005**, *58*, 11.
33. Pičerko Peklar, S. Ovadba zaradi smrdljive lagune. *Večer* **2014**, *70*, 7.
34. Pičerko Peklar, S. Navidez prijetna, v resnici nevarna laguna pod jezom Ptujskega jezera. *Večer* **2017**, *73*, 15.
35. Siivola, J.; Schmid, R. A Systematic Nomenclature for Metamorphic Rocks: 12. List of Mineral Abbrevations. Recommendations by the IUGS Subcommission on the Systematics of Metamorphic Rocks: Web Version. 2007. Available online: https://www.bgs.ac.uk/ (accessed on 1 February 2020).
36. Golden Software. *Grapher*, version 11; Golden Software, LLC: Golden, CO, USA, 2025.
37. Golden Software. *Surfer*, version 8.0; Golden Software, LLC: Golden, CO, USA, 2025.
38. TIBCO. *Statistica*, version 13.3; TIBCO Software, Inc.: Palo Alto, CA, USA, 2017.
39. Sinex, S.A.; Helz, G.R. Regional geochemistry of trace elements in Chesapeake Bay sediments. *Environ. Geol.* **1981**, *3*, 315–323. [CrossRef]
40. Taylor, S.; McLennan, S. *The Continental Crust: Its Composition and Evolution*; Blackwell: Oxford, UK, 1985; p. 312.

41. Yongming, H.; Peixuan, D.; Junji, C.; Posmentier, E.S. Multivariate analysis of heavy metal contamination in urban dusts of Xi'an, Central China. *Sci. Total Environ.* **2006**, *355*, 176–186. [CrossRef]
42. Mueller, G. Index of geoaccumulation in sediments of the Rhine River. *Geojournal* **1969**, *2*, 108–118.
43. OG RS, no. 68/96. Uredba o Mejnih, Opozorilnih in Kritičnih Imisijskih Vrednostih Nevarnih Snovi v Tleh. Available online: https://pisrs.si/pregledPredpisa?id=URED114 (accessed on 23 July 2020).
44. ESDAT. Dutch Target and Intervention Values (2000) (the New Dutch List). Annexes. Circular on Target Values and Intervention Values for Soil Remediation. Ministry of Housing, Spatial Planning and the Environment. 2000. Available online: http://www.esdat.com.au (accessed on 23 July 2020).
45. Council Directive 86/278/EEC of 12 June 1986 on the Protection of the Environment, and in Particular of the Soil, When Sewage Sludge is Used in Agriculture. Available online: https://eur-lex.europa.eu/legal-content/EN/TXT/?uri=celex%3A31986L0278 (accessed on 23 July 2020).
46. Rothe, M.; Kleeberg, A.; Hupfer, M. The occurrence, identification and environmental relevance of vivianite in waterlogged soils and aquatic sediments. *Earth-Sci. Rev.* **2016**, *158*, 51–64. [CrossRef]
47. Ciszewski, D.; Grygar, T.M. A Review of Flood-Related Storage and Remobilization of Heavy Metal Pollutants in River Systems. *Water Air Soil Pollut.* **2016**, *227*, 239. [CrossRef]
48. Schulz Zunkel, C. Trace Metal Dynamics in Floodplain Soils. A Case Study with the River Elbe in Germany. Doctoral Dissertation, Faculty of Mathematics and Natural Sciences, Christian-Albrechts University of Kiel, Kiel, Germany, 23 November 2014.
49. Zawadzki, D.; Maciąg, Ł.; Abramowski, T.; McCartney, K. Fractionation Trends and Variability of Rare Earth Elements and Selected Critical Metals in Pelagic Sediment from Abyssal Basin of NE Pacific (Clarion-Clipperton Fracture Zone). *Minerals* **2020**, *4*, 320. [CrossRef]
50. Hindersmann, I.; Mansfeldt, T. Trace element solubility in multimetal-contaminated soil as affect by redox conditions. *Water Air Soil Pollut.* **2014**, *225*, 2158. [CrossRef]
51. Pavlović, P.; Marković, M.; Kostić, O.; Sakan, S.; Đorđević, D.; Perović, V.; Pavlović, D.; Pavlović, M.; Čakmak, D.; Jarić, S.; et al. Evaluation of potentially toxic element contamination in the riparian zone of the River Sava. *Catena* **2019**, *174*, 399–412. [CrossRef]
52. Tang, Q.; Bao, Y.; He, X.; Zhou, H.; Cao, Z.; Gao, P.; Zhong, R.; Hu, Y.; Zhang, X. Sedimentation and associated trace metal enrichment in the riparian zone of the Three Gorges Reservoir, China. *Sci. Total Environ.* **2014**, *479–480*, 258–266. [CrossRef] [PubMed]
53. Brenčič, M.; Keršmanc, T.; Dolžan, E.; Vidmar, I.; Torkar, A. *Geološki Pogled na Vzroke in Posledice Poplav Leta 2012 na Ptujskem Polju*; Zavod za ribištvo Slovenije: Ljubljana, Slovenia, 2013; pp. 33–39.
54. Polajnar, J. Visoke vode v Sloveniji leta 1998. *UJMA* **1999**, *13*, 143–150.
55. Suhadolnik, A. *Težave Vzdrževanja na Dravi od Maribora do Zavrča*; Zavod za ribištvo Slovenije: Ljubljana, Slovenia, 2001.
56. Pičerko Peklar, S. Obremenjen svet ob Dravi. *Večer* **2013**, *69*, 23.
57. Tribovillard, N.; Riboulleau, A.; Lyons, T.; Baudin, F. Enhanced trapping of molybdenum by sulfurized marine organic matter of marine origin in Mesozoic limestones and shales. *Chem. Geol.* **2004**, *213*, 385–401. [CrossRef]
58. Ye, L.; Meng, X.; Jiang, C. Influence of sulfur on the mobility of arsenic and antimony during oxic-anoxic cycles: Differences and competition. *Geochim. Cosmochim. Acta* **2020**, *288*, 51–67. [CrossRef]
59. Labrenz, M. Formation of Sphalerite (ZnS) Deposits in Natural Biofilms of Sulphate Reducing Bacteria. *Science* **2000**, *290*, 1744–1747. [CrossRef]
60. Du Laing, G.; Rinklebe, J.; Vandecasteele, B.; Meers, E.; Tack, F.M.G. Trace metal behaviour in estuarine and riverine floodplain soils and sediments: A review. *Sci. Total Environ.* **2009**, *407*, 3972–3985. [CrossRef] [PubMed]
61. Kohl, D.; Shearer, G.; Commoner, B. Variation of 15N in Corn and Soil Following Application of Fertilizer Nitrogen. *Soil Sci. Soc. Am. J.* **1973**, *37*, 888–892. [CrossRef]
62. Makarov, M.I. The nitrogen isotopic composition in soils and plants: Its use in environmental studies (A Review). *Eurasian Soil Sci.* **2009**, *42*, 1335–1347. [CrossRef]
63. Nikolenko, O.; Jurado, A.; Borges, A.; Knoeller, K.; Brouyere, S. Isotopic composition of nitrogen species in groundwater under agricultural areas: A review. *Sci. Total Environ.* **2018**, *621*, 1415–1432. [CrossRef]
64. Rogers, K.; Turnbull, R.; Martin, A.; Baisden, W.; Rattenbury, M. Stable isotopes reveal human influences on southern New Zealand soils. *Appl. Geochem.* **2017**, *82*, 15–24. [CrossRef]
65. Cravotta, C. *Use of Stable Isotopes of Carbon, Nitrogen, and Sulfur to Identify Sources of Nitrogen in Surface Waters in the Lower Susquehanna River Basin, Pennsylvania*; US Geological Survey Water Supply Paper; U.S. Geological Survey: Washington, DC, USA, 1997; Volume 2497.
66. Hobbie, E.A.; Ouimette, A.P. Controls of nitrogen isotope patterns in soil profiles. *Biogeochemistry* **2009**, *95*, 355–371. [CrossRef]
67. Trandel, M.A.; Vigardt, A.; Walters, S.A.; Lefticariu, M.; Kinsel, M. Nitrogen Isotope Composition, Nitrogen Amount, and Fruit Yield of Tomato Plants Affected by the Soil–Fertilizer Types. *ACS Omega* **2018**, *3*, 6419–6426. [CrossRef] [PubMed]
68. Högberg, P. Tansley Review No. 95 15N natural abundance in soil-plant systems. *New Phytol.* **1997**, *137*, 179–203. [CrossRef]

69. Karamanos, R.; Rennie, D. Changes in natural 15N abundance associated with pedogenic processes in soil: Changes associated with saline seeps. *Can. J. Soil Sci.* **1980**, *60*, 337–344. [CrossRef]
70. Zhao, B.; Maeda, M.; Ozaki, Y. Natural 15N and 13C Abundance in Andisols Influenced by Long-Term Fertilization Management in Japan. *J. Soil Sci. Plant Nutr.* **2002**, *48*, 555–562. [CrossRef]
71. Reimann, C.; Birke, M.; Demetriades, A.; Filzmoster, P.; O'Connor, P. *Chemistry of Europe's Agricultural Soils; Part A: Methodology and Interpretation of the GEMAS Data Set*; Bundesanstalt für Geowissenschaften und Rohstoffe (BGR): Hannover, Germany, 2014; p. 523.
72. Richards, J.R.; Zhang, H.; Schroder, J.L.; Hattey, J.A.; Raun, W.R.; Payton, M.E. Micronutrient Availability as Affected by the Long-Term Application of Phosphorus Fertilizer and Organic Amendments. *Soil Sci. Soc. Am. J.* **2011**, *75*, 927–939. [CrossRef]
73. Trep, A. Problematika Komunalnega Blata v Čistilni Napravi Ptuj. Bachelor's Thesis, Univerza v Mariboru, Maribor, Slovenia, September 2016.
74. Ning, C.; Gao, P.; Wang, B.; Lin, W.; Jiang, N.; Cai, K. Impacts of chemical fertilizer reduction and organic amendments supplementation on soil nutrient, enzyme activity and heavy metal content. *J. Integr. Agric.* **2017**, *16*, 1819–1831. [CrossRef]
75. Cabilovski, R.; Manojlović, M.; Bogdanovic, D.; Magazin, N.; Keserovic, Z.; Sitaula, B. Mulch type and application of manure and composts in strawberry (Fragaria × ananassa Duch.) production: Impact on soil fertility and yield. *Zemdirb.-Agric.* **2014**, *101*, 67–74. [CrossRef]
76. Prabhu, M.; Mutnuri, S. Cow urine as a potential source for struvite production. *Int. J. Recycl. Org. Waste Agric.* **2014**, *3*, 49. [CrossRef]
77. Inštitut za varstvo okolja Maribor. *CRP: Priprava Okoljskih Standardov za Kemijske Snovi v Vodnem Okolju: Poročilo I Faze Projekta: Priprava Seznama za Vodno Okolje Relevantnih Snovi*; Inštitut za varstvo okolja Maribor: Maribor, Slovenia, 2005.
78. Zheng, H.; Zhang, C.; Liu, B.; Liu, G.; Zhao, M.; Xu, G.; Luo, X.; Li, F.; Xing, B. Biochar for Water and Soil Remediation: Production, Characterization, and Application. In *A New Paradigm for Environmental Chemistry and Toxicology: From Concepts to Insights*; Jiang, G., Li, X., Eds.; Springer: Singapore, 2020; pp. 153–196.
79. Rascio, N.; Navari-Izzo, F. Heavy metal hyperaccumulating plants: How and why do they do it? And what makes them so interesting? *Plant Sci.* **2011**, *180*, 169–181. [CrossRef] [PubMed]